

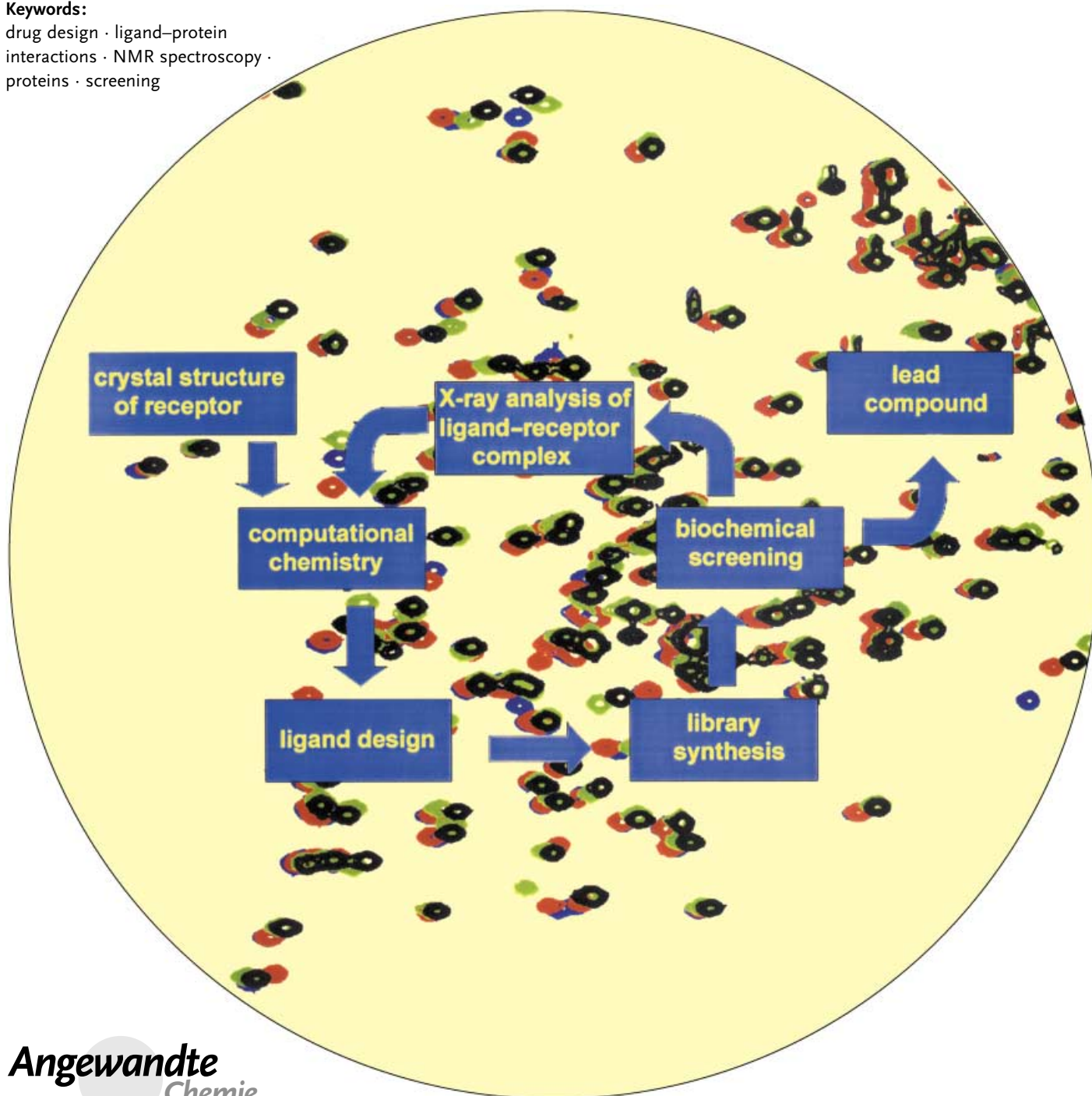
## NMR Spectroscopy of Biomolecules

## NMR Spectroscopy Tools for Structure-Aided Drug Design

Steve W. Homans\*

## Keywords:

drug design · ligand–protein interactions · NMR spectroscopy · proteins · screening



**B**iomolecular NMR spectroscopy has expanded dramatically in recent years and is now a powerful tool for the study of structure, dynamics, and interactions of biomolecules. Previous limitations with respect to molecular size are no longer a primary barrier, and systems as large as 900 kDa were recently studied. NMR spectroscopy is already well-established as an efficient method for ligand screening. A number of recently developed techniques show promise as aids in structure-based drug design, for example, in the rapid determination of global protein folds, the structural characterization of ligand–protein complexes, and the derivation of thermodynamic parameters. An advantage of the method is that all these interactions can be studied in solution—time-consuming crystallization is not necessary. This Review focuses on recent developments in NMR spectroscopy and how they might be of value in removing some of the current “bottle-necks” in structure-based drug discovery.

## 1. Introduction

The Human Genome Sequence project is providing a wealth of information on the products of gene expression, many of which have unknown function. The identification of the roles of these molecules and their interactions in the homeostasis of the cell will offer unprecedented opportunities for therapeutic intervention in disease. Similarly, the increasing numbers of pathogens whose genome sequences have now been described will open new avenues for the development of new antibiotics. This in turn has given rise to a dramatic expansion in the requirement for the 3D structures of proteins. Given the widening gap between the number of protein structures currently solved and the number of available protein sequences, it follows that rapid, robust methods for the determination of protein global folds are urgently required.

From the point of view of structure-based drug design, structure determination is only part of the process that gives rise to suitable lead compounds, as illustrated in the generic iterative cycle of Figure 1. This cycle of design, synthesis, evaluation, and structural analysis involves the determination

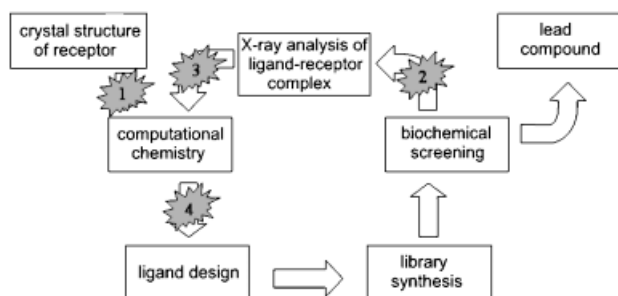


**Figure 1.** Iterative cycle for the discovery of lead compounds with some “bottle-necks”. New NMR-based methods are ideally suited to improve the efficiency of 1) protein-structure determination, 2) ligand screening, 3) structural analysis of ligand–protein complexes, and 4) ligand design.

## From the Contents

1. Introduction	291
2. Determination of Protein Structure	291
3. Ligand Screening	294
4. Determination of Structures of Complexes	295
5. Molecular Dynamics and Ligand Design	297
6. Summary and Outlook	299

of the structure of not only the protein target (or ideally the complex of the target with the natural ligand) but also a significant number of ligand–receptor complexes. Moreover, a suitable screening method is required to identify “active ligands”, and ideally an understanding of the molecular basis of ligand affinity and specificity is required. It is not surprising given these requirements that a number of “bottle-necks” can occur in this cycle. With the advent of very powerful new methods based on NMR spectroscopy, the possibility now exists to overcome many of these difficulties. Specifically, NMR spectroscopic methods are now well-suited to address the four main aspects of the iterative cycle highlighted in Figure 1. An appraisal of these methods forms the subject of this review, with the focus principally on developments in the last decade. I apologize to those whose substantial earlier contributions are not accredited directly herein but which have already been reviewed adequately elsewhere.<sup>[1–8]</sup>

## 2. Determination of Protein Structure

### 2.1. The Problem

Despite a number of very significant advances in both protein crystallography and biomolecular NMR spectroscopy in recent years, the determination of the 3D structures of all but the smallest macromolecules is far from routine. Problems with protein overexpression aside, it is very difficult to predict a timescale for the production of diffraction-quality crystals of a given protein, and in the case of certain membrane proteins it is possible that this cannot be achieved at all in the foreseeable future. Although NMR-based approaches to

[\*] Prof. S. W. Homans  
School of Biochemistry and Molecular Biology  
University of Leeds  
Leeds, LS2 9JT (UK)  
Fax: (+44) 113-343-3167  
E-mail: s.w.homans@leeds.ac.uk

protein-structure determination do not suffer from this limitation, historically there are a number of significant obstacles to the use of this technique in a robust and automated manner. Foremost amongst these is the need to assign a substantial fraction of the resonances observed in NMR spectra in order to generate a list of pairwise nuclear Overhauser effect (NOE) distance restraints with which to determine the 3D structure of the molecule. It is well known that ideally ten or more such restraints per residue (amino acid) are required to obtain a “good” 3D structure. This restraints list will include side-chain- as well as backbone-derived restraints, and thus by definition side-chain resonance assignments are required—a time-consuming task that is not well-suited to automation. However, from the point of view of functional genomics, the determination of the protein global fold is, in principle, sufficient for the assignment of gene function based on 3D structure homology. Whereas a global fold is clearly insufficient for lead optimization, for which atomic-resolution structures are generally required, low-resolution structures may be adequate for “SAR by NMR” type screening, in which the protein is assigned but no 3D structure is available.

## 2.2. NOE-Based Methods

Given the time-consuming nature of side-chain assignment, it is not surprising that early attempts at the determination of protein global folds focused on the use of NOE restraints from the protein backbone. One of the most successful early attempts was reported by Mal et al.,<sup>[9]</sup> who used 155 backbone amide NOEs and seven tryptophan indole–backbone amide NOEs to determine the global fold of the Fyn SH3 domain. Importantly, the use of a perdeuterated, uniformly <sup>15</sup>N-enriched protein enabled NOE restraints to be measured between amide protons up to 0.7 nm apart, thus giving crucial long-range distance information with which to define the global fold. Despite the fact that only 162 restraints were used in total, a very respectable root mean square deviation (rmsd) for heavy atoms of 0.29 nm was obtained with respect to the crystal structure.

Recognizing that the accuracy of global-fold determination is highly topology-dependent, Kay and co-workers

introduced a strategy based on the selective incorporation of protonated methyl groups in otherwise perdeuterated proteins<sup>[10]</sup> to increase the number of available conformational restraints. This approach with 287 amide–amide, methyl–amide, and methyl–methyl NOE restraints, gave a root mean square deviation (rmsd) of 0.44 nm for heavy atoms of PLCC SH2 domains with respect to the high-resolution solution structure. Overall, however, as indicated by Clore et al.,<sup>[11]</sup> attempts to define global folds using NOE data alone have been only partially successful, with an attainable accuracy between 0.25 and 0.7 nm for the backbone.

## 2.3. RDC-Based Methods

Clore et al. also demonstrated<sup>[11]</sup> that residual dipolar coupling (RDC) measurements can offer a significant improvement in coordinate accuracy when applied as restraints in concert with minimal NOE data sets such as those described in Section 2.2. Unlike NOEs, which provide distance restraints, RDCs provide direct *long-range* angular orientation information.

To see why this is the case, a brief digression into the theory of residual dipolar couplings is necessary. Formally, the dipolar coupling ( $D_{PQ}$ ) between two nuclei P and Q is given by Equation (1), in which  $k$  is a constant that subsumes a

$$D_{PQ}(\theta, \phi) = -\frac{k}{r_{PQ}^3} [A_a(3\cos^2\theta - 1) + \frac{3}{2}A_r\sin^2\theta\cos 2\phi] \quad (1)$$

number of factors that are unimportant for the present discussion,  $r_{PQ}$  is the distance between P and Q,  $A_a$  and  $A_r$  are components of a mathematical function known as the alignment tensor  $\mathbf{A}$ , and  $\theta$  and  $\phi$  are cylindrical coordinates describing the orientation of the vector P–Q in the principal axis system of  $\mathbf{A}$ .

The meaning of this equation can be more easily understood by reference to Figure 2. For the purposes of the present discussion, the principal axis system of the alignment tensor can be thought of as an imaginary cartesian coordinate system that lies adjacent to the molecule of interest. If we now define nuclei P and Q as directly bonded NMR-active nuclei, then



Steve Homans obtained his D.Phil. in Biochemistry at the University of Oxford in 1982. He was a postdoctoral fellow with Prof. Raymond Dwek in Oxford, and thereafter relocated to the University of Dundee as a Lecturer in Biochemistry. In 1996 he became Professor of Biophysical Chemistry at the University of St. Andrews, and was elected Fellow of the Royal Society of Edinburgh in 1997. In 1999 he moved to the University of Leeds where he is now Professor of Structural Biology. His research interests include NMR spectroscopy of carbohydrates and proteins, and the dynamics and thermodynamics of protein–ligand interactions.

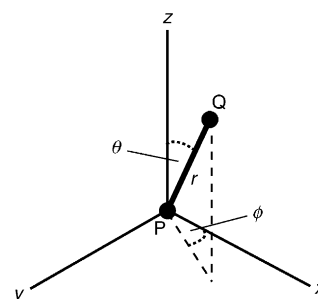


**Figure 2.** Dependence of the residual dipolar coupling  $D_{PQ}$  on the orientation of a bond vector P–Q in terms of cylindrical coordinates ( $r, \theta, \phi$ ) in the principal axis system ( $x, y, z$ ) of the orientation tensor.

the distance  $r_{\text{PQ}}$  will be known since it is the covalent bond length, and the dipolar coupling  $D_{\text{PQ}}$  will depend on the orientation of the bond vector in the imaginary coordinate system (Figure 2). We can also determine  $A_a$ ,  $A_r$ , and the orientation of the coordinate frame by using the observed residual dipolar couplings in the molecule.<sup>[12,13]</sup> Thus if we can measure  $D_{\text{PQ}}$ , then we can determine the orientation of the bond in the coordinate system. Importantly, the measured dipolar coupling for any NMR-active atom pair will be related to the bond-vector orientation with respect to the same imaginary coordinate system. Thus, bond-vector orientations located at opposite ends of a molecule will be related to each other through a common coordinate system, giving rise to the long-range angular orientation information described above. A minor complication that will be addressed later concerns the fact that more than one orientation of the bond vector can give rise to the same value of  $D_{\text{PQ}}$ .

The dipolar coupling is manifested in the NMR spectrum as a splitting of the resonance lines, analogous to scalar ( $J$ ) couplings. However, in isotropic solution, all orientations of the bond vector contribute to the coupling owing to molecular tumbling, and the dipolar coupling averages to zero. In contrast, in the solid state, or under conditions in which the molecule is strongly aligned in some fashion, the dipolar coupling is very strong, and every NMR-active atom in the molecule exhibits a dipolar coupling to every other, despite the  $r^{-3}$  dependence of the interaction. The result is a spectrum that is impossible to interpret. Thus, to be of use for macromolecules, a method is required by which the molecule can be *weakly* aligned. Such a system was discovered by Tjandra and Bax, who realized that these dipolar couplings can be measured in dilute liquid-crystalline media.<sup>[14]</sup> Due to the weak alignment induced by these media, the observed dipolar couplings are a fraction of the strength of those observed in highly aligned systems, and are thus referred to as residual dipolar couplings (RDCs). Since the original observation of Tjandra and Bax, many such media appropriate for biological systems have now been described.<sup>[15–22]</sup> The availability of more than one medium is very important as the orientation of a given molecule will generally not be the same in two different media. This phenomenon can be used to overcome difficulties with multiple possible orientations of bond vectors mentioned above—it can be shown mathematically that the simultaneous solution of the dipolar coupling equation in two different alignment media (i.e. different alignment tensors) gives rise in general to a single unambiguous vector orientation.<sup>[23,24]</sup>

As RDCs can be measured in a straightforward fashion from splittings in NMR spectra, it is unsurprising that much attention has been focused in recent years on their use in protein global-fold determination. Mueller et al. developed a methodology for orienting peptide planes by using dipolar couplings, which was utilized to determine the global fold of maltose-binding protein in complex with  $\beta$ -cyclodextrin. This gave rise to pairwise rmsd values between N- and C-terminal domains of the NMR structure and the corresponding regions in the X-ray structure of 0.28 nm and 0.31 nm, respectively.<sup>[25,26]</sup> Fowler et al.<sup>[27]</sup> used  $N_i-H_i^N$ ,  $H_i^N-H_i^\alpha$ ,  $H_i^N-H_{i+1}^\alpha$ ,  $H_i^N-H_{i+1}^N$  residual dipolar couplings together with a small

number of backbone–side-chain NOEs to determine the backbone fold of the acyl-carrier protein to an rmsd between backbone atoms of 0.3 nm. Moreover, Hus et al.<sup>[28]</sup> used long-range order restraints available from paramagnetic systems in combination with residual dipolar couplings to define the fold of cytochrome  $c'$  in the complete absence of NOE restraints. Recently, the same group determined the global fold of ubiquitin to 0.1 nm rmsd for the backbone (residues 1–71)<sup>[29]</sup> with respect to the solution structure determined by conventional methods, using restraints derived solely from  $N_i-H_i^N$ ,  $C_{i-1}'-N_i$ ,  $C_{i-1}'-H_i^N$ ,  $C_i^\alpha-C_i'$ ,  $C_i^\alpha-H_i^\alpha$ , and  $C_i^\alpha-C_i^\beta$  residual dipolar couplings in two independent tensor frames. Excellent results were also obtained by use of residual dipolar couplings in concert with molecular fragment replacement.<sup>[30–33]</sup> Interesting recent developments include single-step determination of protein substructures<sup>[34]</sup> from residual dipolar couplings and simultaneous resonance assignment.<sup>[35]</sup>

Thus it can be seen that use of residual dipolar couplings either alone or in concert with a limited subset of NOE restraints can dramatically increase the accuracy of global-fold determination. Very recently, Giesen et al. demonstrated that it is possible to define the global fold of ubiquitin to an rmsd of 0.14 nm with respect to the crystal structure using only backbone residual dipolar coupling ( $N_i-H_i^N$ ,  $N_i-C_{i-1}'$ ,  $H_i^N-C_{i-1}'$ ) and amide–amide NOE restraints<sup>[36]</sup> (Figure 3). Importantly,



**Figure 3.** Stereoview of the global fold of human ubiquitin determined by using backbone residual dipolar coupling restraints and long-range amide–amide NOE restraints (black) compared with the crystal structure (grey).<sup>[36]</sup>

tantly, this approach is compatible with both perdeuteration<sup>[37]</sup> and selective backbone isotopic enrichment<sup>[38,39]</sup> and thus offers optimal sensitivity for larger proteins. The relative ease with which backbone resonance assignments can be obtained (in contrast to side-chain assignments) suggests that this approach may offer a very rapid route to global-fold determination.

The efficacy of this and other approaches for global-fold determination involving residual dipolar couplings is, however, likely to depend on topology. In proteins that contain a high  $\alpha$ -helical content, it is likely that long-range amide NOE restraints will be sparse. In general, long-range NOEs are vital for correct fold determination because they introduce translational position information that is not contained in RDCs (unless all residue positions are defined precisely and uniquely). However, a small number of such NOEs may be sufficient. For example, Prestegard and co-workers<sup>[27]</sup> were able to derive the global fold of the acyl-carrier protein of

*E. coli* by use of residual dipolar coupling measurements together with one backbone–backbone NOE and four backbone–side-chain NOEs. Similarly, the same authors determined the global fold of the NodF protein of *Rhizobium leguminosarum* with five backbone–backbone NOEs.

Clearly, the use of NOEs involving side-chain atoms requires the assignment of the latter, which could, in principle, dramatically increase the time required for the derivation of a global fold. However, since the number of required NOEs would appear to be small, the effort required for assignment can be reduced by careful choice of isotopic-labeling strategies based on residue type, in a manner analogous to that introduced by Kay and co-workers (Section 2.2).<sup>[10,40–43]</sup> Moreover, the recent demonstration that  $^1\text{H}$ – $^1\text{H}$  residual dipolar couplings can provide distance restraints of up to 0.7 nm in ubiquitin<sup>[44]</sup> suggests an alternative source of long-range restraints for global-fold determination.

## 2.4. Outlook

The use of residual dipolar couplings in concert with sparse NOE restraints offers a very promising route to the determination of protein structures at low to medium resolution. These structures will be entirely adequate for many structural genomics applications and for NMR-based screening. The barrier to obtaining high-resolution structures using this approach lies in the requirement for additional conformational restraints. This, in turn, dramatically increases the time and effort required to obtain the necessary resonance assignments. In this regard there is clearly significant potential for further optimization of isotopic-labeling strategies to facilitate and ideally automate this process.

## 3. Ligand Screening

### 3.1. The Problem

Ligand design is an imprecise art. One reason for this is that, despite enormous advances in techniques for structure determination, our knowledge of the factors that govern affinity and specificity of biomolecular interactions is very rudimentary. Fundamental thermodynamics tells us that the affinity is not governed by structure alone, but is a complex interplay between structure and dynamics (see Section 5). Thus, although a high-resolution structure of the ligand–protein complex is unquestionably thought-provoking in the context of ligand design, the probability that an effective lead compound can be designed on the basis of this structure is very small. One way to overcome this deficiency is to synthesize not one ligand, but many diverse ligands based on a common scaffold, that is, a focused combinatorial library. This gives rise to the need for a suitable screening assay. The NMR chemical shift is an exquisitely sensitive probe of chemical environment and hence biomolecular interaction, and a number of effective NMR-based screening techniques have been described in recent years. These are outlined

briefly below. The reader is referred to the recent review of Meyer and Peters for a more detailed account of these methods.<sup>[45]</sup>

### 3.2. Methods Based on Protein Resonances

One of the simplest yet most effective NMR-based screening strategies, introduced by Fesik and co-workers, is 2D  $^1\text{H}$ ,  $^{15}\text{N}$ -heteronuclear single quantum coherence (HSQC) spectroscopy.<sup>[46–48]</sup> By uniformly enriching the protein with  $^{15}\text{N}$ , which is usually straightforward and inexpensive, only the protein resonances are visible in such spectra, and hence the candidate ligand (or ligands, which could be small molecules or other macromolecules) can be included at relatively high concentrations. By comparison of the HSQC spectra of a reference spectrum of the ligand-free protein with a similar spectrum acquired in the presence of ligand(s), information on binding can be obtained from the resonance shifts between the two spectra. A number of candidate ligands, typically ten, can be included in any given sample, and the active ligand can be deconvoluted by further HSQC experiments if a “hit” is obtained. The chemical shifts of protein amide resonances are very sensitive to bound ligands and hence the HSQC approach is a very effective method for the assay of ligands that bind only very weakly ( $K_d \leq 1 \text{ mM}$ ).

Shuker et al.<sup>[46]</sup> used this method to advantage in a lead-generation approach that effectively covalently links two weakly binding ligands located in adjacent binding sites. Clearly, structural information on the protein is required to apply this technique—in the absence of a crystal structure, an NMR-derived global fold may be sufficient (see Section 2).

Figure 4 illustrates the extreme sensitivity of the HSQC approach. This figure shows a superimposition of the  $^1\text{H}$ ,  $^{15}\text{N}$ -HSQC spectra of a number of related pyrazine ligands bound to a sample of uniformly  $^{15}\text{N}$ -enriched mouse major urinary protein. In this example, both resonance assignments<sup>[49]</sup> and crystal structures<sup>[50,51]</sup> are available for the protein, so that it is

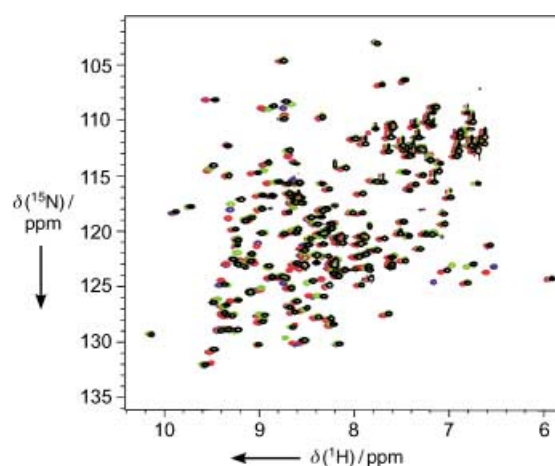


**Figure 4.** Overlaid  $^1\text{H}$ ,  $^{15}\text{N}$ -HSQC spectra of uniformly  $^{15}\text{N}$ -enriched mouse major urinary protein bound to four related ligands. Blue: 2-methoxypyrazine, red: 2-methoxy-3-methylpyrazine, green: 3-isopropyl-2-methoxypyrazine, black: 3-isobutyl-2-methoxypyrazine.

a simple matter to identify binding-site residues. By measuring shift differences between spectra,<sup>[52]</sup> it is also possible to obtain information on the locations of the various aliphatic side chains of the various ligands within the binding site, which agree closely with structural data for related ligands.<sup>[51,53]</sup>

In terms of simplicity, ease of use, and affordability, the HSQC approach would appear to be a very attractive route to ligand screening. Although this technique is in no way a “high-throughput” approach, it is particularly valuable for screening weakly-binding ligands, which can readily be missed in conventional biochemical assays. Moreover, straightforward measurement of chemical shift changes versus ligand concentration<sup>[54]</sup> or application of diffusion-based methods<sup>[55]</sup> enables ligand-binding constants to be measured.

A related approach for ligand screening involves  $^{13}\text{C}$  isotopic enrichment of methyl groups on protein side chains. Although  $^{13}\text{C}$  isotopic enrichment would typically be considered prohibitively expensive for screening purposes, given the relatively large amounts of protein required, Fesik and co-workers devised an ingenious approach for the selective  $^{13}\text{C}$  labeling of side-chain methyl groups by using inexpensive  $^{13}\text{CH}_3\text{I}$ .<sup>[56]</sup> A major advantage of this  $^{13}\text{CH}_3$ -based screening is that  $^1\text{H}$ ,  $^{13}\text{C}$ -HSQC is considerably more sensitive than  $^1\text{H}$ ,  $^{15}\text{N}$ -HSQC for a given sample concentration. Typically, threefold higher sensitivity is obtained for proteins < 30 kDa, enabling  $^1\text{H}$ ,  $^{13}\text{C}$ -HSQC spectra to be acquired on a 50  $\mu\text{M}$  sample of protein in 10 min. Moreover, the use of selective methyl labeling in combination with deuterium enrichment enables screening of protein targets in excess of 100 kDa. The availability of cryoprobe technology at intermediate to high fields promises to widen still further the scope for NMR-based screening, with the possibility of natural-abundance  $^{13}\text{C}$  spectroscopy on the horizon.

### 3.3. Methods Based on Ligand Resonances

While very effective, the approaches described in Section 3.2 do not provide any information on which ligand binds to the target protein, except in trivial cases in which only one ligand is present in a given sample. Moreover, no information is obtained on the “active” chemical groupings of the ligands that are located in and interact with the binding site of the target protein. However, this information can be derived with NMR spectroscopy by using NMR techniques that detect ligand resonances.

One simple approach to detect which ligand (out of a small set of (typically) ten ligands) undergoes binding is to exploit the difference in the relaxation properties or translational diffusion coefficient of the free ligand with when it binds to the target protein. This can be achieved by using simple 1D NMR experiments designed to measure  $T_2$  relaxation times or diffusion coefficients.<sup>[57]</sup> A related technique exploits the fact that NOEs for bound ligands are typically large and negative whereas for free ligands they are very small.<sup>[58]</sup> In the fast-exchange regime, that is, relatively weak binding, these so-called transferred NOEs (TRNOEs) can readily be measured by using homonuclear 2D NMR

techniques. Importantly, it is not necessary to isotopically enrich either the ligand or the protein in order to record these data. This is because it is possible to work with relatively high ligand/protein ratios (typically 15:1), whereby the relatively narrow ligand resonances can easily be observed above the much broader background protein resonances.

To determine the “active” regions of a given ligand, a simple 1D NMR experiment termed saturation transfer difference (STD) can be applied.<sup>[59,60]</sup> This technique relies on the fact that in large complexes, proton magnetization is very efficiently transferred throughout the molecule or molecules owing to a process known as spin diffusion. Hence, if a region of the NMR spectrum of the complex containing resonances for the protein (but not for the ligand) is saturated (i.e. the magnetization is attenuated) by application of a radiofrequency field, this saturation will be efficiently transferred through the protein and also to resonances of the ligand that are located within the protein-binding site. This technique has proven remarkably successful at mapping the active regions of ligands and can also be used as a simple screening tool.

One situation in which the above approaches might fail concerns ligands that bind strongly to the protein of interest. Under these circumstances, the chemical-exchange phenomena on which the above methods depend are not on the appropriate timescales. However, under these circumstances, NMR reporter screening can be applied. The basis of this approach is quite straightforward: During acquisition of spectra of the free protein and of the protein in the presence of ligand(s), a “reporter-ligand” that is known to bind weakly to the protein is also included. When a ligand that binds more tightly than the reporter ligand is present in the sample, the binding event can be detected by changes in intensity and line-width of the latter—these will change as the fraction of free reporter ligand in solution increases as it is displaced from the binding site of the protein.<sup>[61,62]</sup>

### 3.4. Outlook

NMR-based screening is now an established tool in structure-based drug design. One field that is likely to benefit greatly from NMR approaches is “interactome” research, that is, characterization of protein–protein interactions in the genome. With the recent spectacular demonstration by Wuthrich and co-workers that interactions within the 900-KDa complex of GroEL–GroES can be studied<sup>[63]</sup> by using transverse relaxation optimized spectroscopy (TROSY),<sup>[64]</sup> molecular size is unlikely to limit the future usefulness of NMR spectroscopy in this application.

## 4. Determination of Structures of Complexes

### 4.1. The Problem

The lead discovery and optimization cycle of Figure 1 requires that the structures of a number of candidate ligand–protein complexes are solved. This necessarily must be done



as rapidly as possible. In this respect X-ray crystallography, although capable of providing high-resolution structures, is not ideal owing to the difficulty in predicting the timescale of crystallization of these complexes. High-resolution NMR spectroscopy offers a useful alternative, not least because it is possible to determine, from simple trial experiments, whether structure determination of a given complex is achievable, and an approximate timescale for the process. However, the NMR approach has in the past suffered from a number of limitations. Described below are a number of recent techniques designed to overcome these challenges.

#### 4.2. NOE-Based Methods

Intuitively, the most obvious approach to structure determination of ligand–protein complexes involves NOE-based distance restraints in a manner analogous to protein-structure determination. However, many of the NOEs are intermolecular in nature and hence a number of useful approaches can be used to simplify the problem of identifying these NOEs from amongst the plethora of intramolecular NOEs from the protein. Essentially, these approaches all rely on the fact that only the protein or the ligand is isotopically enriched. As the former is much easier to achieve by using recombinant DNA technology, the majority of techniques have been designed accordingly.

Early experiments<sup>[65,66]</sup> utilized  $^{15}\text{N}$ -enriched proteins and enabled the selective observation of NOEs between protons attached to  $^{15}\text{N}$  and protons attached to  $^1\text{H}$ , thus suppressing both protein–protein and ligand–ligand NOEs. Whereas the selection of protons attached to  $^{15}\text{N}$  or  $^{13}\text{C}$  (isotope editing) is very straightforward in a background that contains a natural abundance of  $^{15}\text{N}$  or  $^{13}\text{C}$ , this is not true for the selection of protons attached to  $^{14}\text{N}$  or  $^{12}\text{C}$  in a background that is  $^{15}\text{N}$  or  $^{13}\text{C}$ . The problem derives from the fact that suppression of protons attached to  $^{15}\text{N}$  or  $^{13}\text{C}$  is achieved by exploiting the scalar one-bond coupling between the proton and the heteronucleus ( $^1J_{\text{N,H}}$  or  $^1J_{\text{C,H}}$ ), whereby the magnetization is “nulled” by using a suitable time delay during the sinusoidal evolution of magnetization under the influence of this coupling. Unfortunately, scalar couplings differ between chemical groups, and hence a delay that nulls protons of a given type is only partially effective for protons of another type. The net result is that early isotope-filtration experiments with isotopically-enriched proteins suffered from substantial breakthrough of protein-derived magnetization.

These problems have been largely overcome in a series of 3D NMR experiments described by Kay and co-workers,<sup>[67]</sup> who used a novel delay period involving frequency-swept (“chirp”) refocusing pulses to compensate for nonuniform scalar couplings. These techniques are very effective at enabling even weak ligand–protein NOEs to be observed with practically no interfering protein resonances (Figure 5).

In addition to the measurement of intermolecular NOEs, intramolecular NOEs are useful for the determination of the bound-state conformation of the ligand. The simplest approach for the measurement of these NOEs is to use isotope editing in combination with isotopically enriched

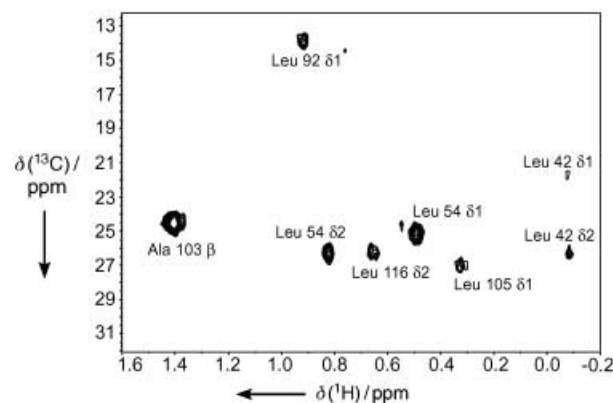


**Figure 5.** 2D plane from the 3D  $^{13}\text{C}$  isotope-filtered NMR spectrum of unlabeled 3-isobutyl-2-methoxypyrazine bound to uniformly  $^{13}\text{C}$ -enriched mouse major urinary protein. The slice is taken at the  $^1\text{H}$  resonance frequency of the magnetically equivalent methyl protons two isobutyl groups. Cross-peaks arise from  $^1\text{H}$ – $^1\text{H}$  NOEs between these methyl protons and the indicated side chains of residues within the binding site of the protein.

ligands.<sup>[68–70]</sup> However, in all but ideal cases, the synthetic effort and isotope costs involved in the preparation of  $^{13}\text{C}$ -enriched ligands is prohibitive. As an alternative, perdeuteration of the protein in combination with homonuclear  $^1\text{H}$  NMR methods enables interligand NOEs to be observed.<sup>[71]</sup> Perdeuteration offers the advantage that large complexes can be determined, since the absence of non-exchangeable protons in the protein significantly reduces transverse relaxation of ligand protons.

#### 4.3. RDC-Based Methods

Despite technical advances such as those described in the previous section, it is impossible to obtain sufficient NOE restraints between a protein and a ligand to define the structure of the complex at a resolution competitive with the best crystal structures. However, the use of RDC measurements promises to revolutionize the technique. As mentioned in Section 2, RDC-based restraints provide long-range orientational information. It is thus possible to determine the bound-state conformation of a ligand in the complete absence of ligand–protein or ligand–ligand NOEs.<sup>[72–74]</sup> Typically, backbone amide  $^{15}\text{N}$ – $^1\text{H}$  RDCs are measured for the protein in a dilute liquid-crystalline medium, and the magnitude and direction of the alignment tensor is determined from these values by using structural coordinates for the protein obtained either by X-ray crystallography or NMR spectroscopy.<sup>[13,75]</sup> Residual dipolar couplings are then measured for the free ligand under the same conditions to obtain the “inherent” RDCs before binding. These will be typically much smaller than those of the protein owing to the much lower degree of alignment observed for small molecules. In most cases, the measurements of choice for the ligand will be one-bond  $^{13}\text{C}$ – $^1\text{H}$  RDCs. To facilitate their measurement, most studies to date have employed  $^{13}\text{C}$ -enriched ligands in combination with isotope editing. Finally, the ligand is combined with the

protein under the same solution conditions, and the ligand RDCs are remeasured. In the case of weak binding, when the protein is not saturated with ligand, the ligand is titrated with the protein and RDC measurements are taken at different ligand/protein ratios. The effective RDC values for the ligand in the complex are then obtained by extrapolation to 100% bound ligand, after subtraction of the inherent RDCs for the free ligand. The bound ligand will adopt the alignment tensor of the protein in the complex and hence the orientation of the ligand with respect to the protein can be determined from the latter RDCs.

One limitation of this approach is that the synthesis of  $^{13}\text{C}$ -enriched compounds can be time-consuming and costly, and is effectively impossible in any practical lead-discovery and optimization strategy. A further disadvantage of this approach is that in the slow-exchange limit (strong binding,  $K_d > 10^{-5}\text{ M}$ ), resonance linewidths become unacceptably large owing to efficient dipolar relaxation between  $^{13}\text{C}$  and  $^1\text{H}$ . Nonetheless, with the availability of cryoprobes for high-field spectrometers, it may be possible to record HSQC spectra of weakly aligned complexes with natural-abundance  $^{13}\text{C}$ , thus enabling RDCs to be measured in unlabeled ligands complexed to  $^{15}\text{N}$ ,  $^2\text{H}$ -enriched proteins.<sup>[76]</sup>

#### 4.4. Outlook

Given the modest time efficiency of X-ray crystallography for solving multiple ligand–protein complex structures, the NMR approach offers a highly attractive alternative. However, it will be necessary to overcome the current size limitation by judicious use of labeling strategies for the protein, which will necessarily involve substantial deuteration. One area that holds particular promise is the use of homonuclear  $^1\text{H}$ – $^1\text{H}$  RDCs<sup>[77–79]</sup> in a perdeuterated protein background, since protons attached to  $^{12}\text{C}$  have workable linewidths under these conditions, even for large complexes.

### 5. Molecular Dynamics and Ligand Design

#### 5.1. Relevance of Dynamics

Although the crystal structure or NMR-derived structure of a protein is unquestionably thought-provoking in the process of lead discovery, the key to understanding the affinity of a ligand for its receptor lies in the dynamics and thermodynamics of the association rather than in a simple static picture. This can be understood by reference to simple concepts in thermodynamics (Figure 6): The Gibbs energy of binding ( $\Delta G_b$ ) of a ligand to a protein is equal to the difference between the free energies of the free species and the free energy of the complex. As a result of the relation  $\Delta G = \Delta H - T\Delta S$ , a flexible ligand (higher conformational entropy) will have a lower Gibbs energy than a rigid ligand. As the standard Gibbs energy of binding is related to affinity by the well-known relation  $\Delta G_b^\circ = -RT \ln K_a = RT \ln K_d$ . It follows that a rigid ligand will bind more tightly than a flexible ligand, all other factors being equal. Exactly the same

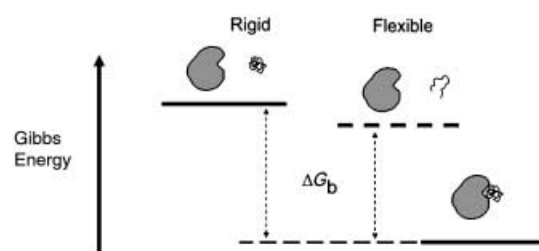


**Figure 6.** Thermodynamic origin of the difference in affinity between a “rigid” ligand and a “flexible” ligand.

argument can be used with respect to “flexible” side chains in the binding sites of proteins.

It thus follows that we must have information on the dynamics (which determine the entropy) of an interaction as well as structural aspects (which determine enthalpy). In a “real” system we must also consider the solvent. With the advent of new technologies such as isothermal titration calorimetry (ITC), it is possible under ideal circumstances to obtain reliable experimental data on the global thermodynamic parameters that govern a biomolecular association. As an example, Table 1 shows ITC-derived thermodynamic parameters for the binding of a series of pyrazine ligands to

**Table 1:** Thermodynamic parameters for the binding of the listed ligands to the mouse major urinary protein determined from isothermal titration calorimetry experiments.

Ligand	$\Delta H^\circ$ [kcal mol <sup>−1</sup> ]	$\Delta S^\circ$ [cal K mol <sup>−1</sup> ]	$\Delta G^\circ$ [kcal mol <sup>−1</sup> ]	$K_d$ [μM]
3-methylpyrazine	−9.99	−16.4	−5.1	185
2-methoxypyrazine	−10.03	−14.5	−5.7	67
2-methoxy-3-methylpyrazine	−8.44	−7.2	−6.3	25
3-isopropyl-2-methoxypyrazine	−9.14	−2.0	−8.53	0.56
3-isobutyl-2-methoxypyrazine	−11.85	−7.4	−9.65	0.08

the mouse major urinary protein. This table illustrates a number of interesting features: 1) The rank order of binding of the ligands differs depending on whether we consider only enthalpy (i.e. no entropy) or Gibbs energy (i.e. with entropy), which further emphasizes the need to consider both structure and dynamics. 2) The difference in Gibbs energy between micromolar and nanomolar dissociation constants is  $\approx 4\text{ kcal mol}^{-1}$ . Thus the difference between a “mediocre” ligand and a “good” ligand equates to approximately one hydrogen bond. 3) These global thermodynamic parameters, while accurately quantifying binding in thermodynamic terms, do not readily tell us why one ligand binds better than another. From the point of view of ligand optimization, it would be of immeasurable benefit to obtain these thermodynamic parameters experimentally on a per-residue rather than on a global basis. In several important recent papers,<sup>[80–83]</sup> new NMR methodologies are described by which standard Gibbs energies and entropies of binding can be derived on a per-residue basis from NMR relaxation data, thus offering a



means by which the thermodynamic behavior of ligand–protein interactions can be characterized at a level of detail that has until now not been possible.

### 5.2. Backbone Dynamics

Isotopic enrichment of proteins enables the measurement of heteronuclear ( $^{15}\text{N}$ ,  $^{13}\text{C}$ , or  $^2\text{H}$ ) relaxation times.<sup>[84]</sup> In general, these heteronuclei are chosen in preference to protons because the latter exhibit very complex relaxation properties under certain circumstances. In particular, uniform  $^{15}\text{N}$  enrichment enables straightforward measurement of amide  $^{15}\text{N}$  relaxation times, which can be used to probe the dynamics of  $\text{N-H}^{\text{N}}$  bond vectors in the protein backbone. These relaxation times are referred to as the longitudinal ( $T_1$ ) and transverse ( $T_2$ ) relaxation times. The reciprocal values  $T_1^{-1}$  and  $T_2^{-1}$  are a measure of the rates of decay of the NMR signal along the direction of the applied magnetic field and transverse to this field, respectively. Just as nuclear spins are excited from one energy level to another in NMR spectroscopy by the application of a radiofrequency field at the resonance frequency, relaxation from a higher energy level to the ground state also requires a magnetic field at the appropriate frequency. These fields derive from local dynamic fluctuations within the molecule, such as overall rotational tumbling and internal motions. Thus, by measurement of relaxation times, we can obtain information on the dynamic events that give rise to relaxation.

NMR relaxation times are usually interpreted in terms of the Lipari–Szabo model-free analysis,<sup>[85]</sup> so named because the relaxation properties can be related to dynamics in a manner that is largely independent of a model for the actual motion. The Lipari–Szabo formalism provides, among others, the square of the so-called generalized order parameter ( $S^2$ ).<sup>[85]</sup> This parameter assumes a value of 1 for a bond vector that is completely immobile and a value of 0 for completely isotropic motion. Importantly, Yang and Kay elegantly showed that within certain well-defined approximations, an analytical relationship exists between the  $S^2$  value for a given bond vector and the conformational entropy of that vector.<sup>[81]</sup> Thus, for example, by measurement of backbone  $^{15}\text{N}$ -relaxation parameters for a given protein in the absence and presence of ligands, differences in  $S^2$  values can be estimated as differences in conformational entropy, that is, entropy of binding, on a per-residue basis. In this manner, details of the thermodynamic behavior of ligand binding are available that cannot be obtained by any other technique.

A number of studies have involved the use of this approach in applications ranging from protein–DNA interactions<sup>[86]</sup> and conformational exchange in calmodulin<sup>[87]</sup> to protein folding.<sup>[81,88]</sup> From the perspective of drug design, an interesting example of the application of this approach concerns ligand binding to the major urinary protein described by Stone and co-workers.<sup>[89]</sup> They observed an increase in protein backbone conformational entropy on ligand binding, and concluded that this term is likely comparable in magnitude to other important Gibbs energy contributions to binding, and may represent a general mechanism in the

binding of small ligands to macromolecules. Clearly, information of this kind is completely obscured in simple static pictures of proteins and protein–ligand complexes, yet may be of paramount importance in governing affinity.

### 5.3. Side-Chain Dynamics

The techniques described in the previous section can similarly be applied to the study of protein side-chain dynamics, with the nucleus of choice being  $^{13}\text{C}$  or  $^2\text{H}$ . In principle,  $^{13}\text{C}$ -based measurements offer higher sensitivity,<sup>[90]</sup> but as discussed at length by Muhandiram et al.,<sup>[91]</sup>  $^2\text{H}$  methods are often preferable in terms of ease of interpretation. However,  $^2\text{H}$  methods do suffer from limitations in terms of molecular mass.<sup>[92]</sup> Most side-chain studies to date have focused on the dynamics of methyl groups. For technical reasons it is preferable to work with  $^{13}\text{CHD}_2$  or  $^{13}\text{CH}_2\text{D}$  isotopomers of methyl groups in  $^{13}\text{C}$ - and  $^2\text{H}$ -relaxation studies, respectively, which gives challenging isotopic-enrichment strategies. Partial isotopic enrichment with  $^2\text{H}$  appears to be the most effective method for obtaining the relevant isotopomers for deuterium-relaxation studies. This can be achieved by overexpression in *E. coli* with uniformly labeled  $^{13}\text{C}$  and 50 %  $^2\text{H}$  enriched glucose as the sole carbon source.<sup>[91]</sup> Recently, useful methods were described by Torchia and co-workers based on protein overexpression in *E. coli* with  $^{13}\text{C}$ ,  $^2\text{H}$ -enriched pyruvate as the sole carbon source.<sup>[92,93]</sup> This approach yields protein samples with high contents of  $\text{CH}_2\text{D}$  and  $\text{CHD}_2$  methyl isotopomers of Ala, Val, Leu, and Ile, which is suitable for both  $^2\text{H}$ - and  $^{13}\text{C}$ -relaxation measurements. Indeed, this approach has enabled a favorable comparison of order parameters of the methyl rotation axes obtained with  $^2\text{H}$  and  $^{13}\text{C}$  measurements on the same sample.<sup>[92]</sup>

A number of studies have employed the above approaches to study side-chain dynamics, with a view to estimating the entropy of rotamer exchange in proteins,<sup>[94]</sup> correlation of dynamics with local structure,<sup>[95]</sup> and the measurement of side-chain entropy changes upon formation of a calmodulin–peptide complex.<sup>[96]</sup> The latter work, discussed in detail by Cavanagh and Akke,<sup>[97]</sup> is potentially of great relevance to structure-based drug design. Importantly, separation was observed between backbone and side-chain response upon ligand binding—there is little change in the motional characteristics of the backbone, but both increases and decreases in entropy are observed along the side chains. In particular, certain side chains remote from the binding site experience increased entropy upon binding, thus negating, in part, the entropic penalty experienced upon ligand binding by other side chains within the binding site.

### 5.4. Outlook

Quantitative studies on protein backbone and side-chain entropies with NMR relaxation measurements are still at an early stage, but the results thus far are extremely encouraging. It does appear possible to obtain reasonable estimates of

protein backbone and side-chain entropy differences upon ligand binding that agree with global thermodynamic data measured by other methods. In this respect, NMR techniques can potentially supply the missing piece in the thermodynamic “jigsaw puzzle” that characterizes ligand binding. The number of such studies is too small as yet to determine whether any patterns will emerge, but given the importance of entropy, or more particularly enthalpy–entropy compensation in biological recognition phenomena,<sup>[98–100]</sup> further work in this area is certainly warranted.

## 6. Summary and Outlook

Two decades ago NMR spectroscopy was regarded as a technique restricted to “small” molecules. Since that time, the technique has developed at an enormous pace—structure determinations of proteins in the 30–40-kDa range are becoming routine, and with the advent of higher magnetic fields, cryoprobe technology, and advances in isotopic-enrichment strategies, it is very likely that molecular mass will cease to be the major limitation. As a method that can simultaneously offer a route to determine structure, to screen ligands, and to probe dynamics, it is perhaps surprising that the approach has not been more widely used in the drug-discovery arena. However, many of the advances described in this Review are quite recent, and naturally it will take some time for these to be validated and accepted by the pharmaceutical industry. Of the applications described, the determination of per-residue entropy terms for a given biomolecular interaction is perhaps the most intriguing. Unlike protein crystallography, which can very usefully be applied in parallel to the NMR approach for structure determination and (increasingly) for ligand screening, NMR methods are uniquely able to provide this high-resolution “dynamic” picture of the interaction. Of course, the contribution of solvent is also potentially an important factor that governs affinity, but recent developments in nuclear magnetic relaxation dispersion measurements offer promise in this direction.<sup>[101]</sup>

*The author gratefully acknowledges financial support from the Biotechnology and Biological Sciences Research Council (BBSRC) and the Wellcome Trust.*

Received: February 7, 2003 [A581]

- [1] J. H. Prestegard, H. Valafar, J. Glushka, F. Tian, *Biochemistry* **2001**, *40*, 8677.
- [2] M. Sattler, J. Schleucher, C. Griesinger, *Prog. Nucl. Magn. Reson. Spectrosc.* **1999**, *34*, 93.
- [3] G. M. Clore, A. Gronenborn, *Curr. Opin. Chem. Biol.* **1998**, *2*, 564.
- [4] A. M. Gronenborn, G. M. Clore, *Crit. Rev. Biochem. Mol. Biol.* **1995**, *30*, 351.
- [5] G. M. Clore, A. M. Gronenborn, *J. Protein Chem.* **1994**, *13*, 441.
- [6] A. Bax, S. Grzesiek, *Acc. Chem. Res.* **1993**, *26*, 131.
- [7] G. M. Clore, A. M. Gronenborn, *Science* **1991**, *252*, 1390.
- [8] M. Pellecchia, D. S. Sem, K. Wüthrich, *Nat. Rev. Drug Discovery* **2002**, *1*, 211.
- [9] T. K. Mal, S. J. Matthews, H. Kovacs, I. D. Campbell, J. Boyd, *J. Biomol. NMR* **1998**, *12*, 259.
- [10] K. H. Gardner, M. K. Rosen, L. E. Kay, *Biochemistry* **1997**, *36*, 1389.
- [11] G. M. Clore, M. R. Starich, C. A. Bewley, M. L. Cai, J. Kuszewski, *J. Am. Chem. Soc.* **1999**, *121*, 6513.
- [12] G. M. Clore, A. M. Gronenborn, A. Bax, *J. Magn. Reson.* **1998**, *133*, 216.
- [13] J. A. Losonczi, M. Andrec, M. W. F. Fischer, J. H. Prestegard, *J. Magn. Reson.* **1999**, *138*, 334.
- [14] N. Tjandra, A. Bax, *Science* **1997**, *278*, 1111.
- [15] J. A. Losonczi, J. H. Prestegard, *J. Biomol. NMR* **1998**, *12*, 447.
- [16] M. Ottiger, A. Bax, *J. Biomol. NMR* **1998**, *12*, 361.
- [17] R. S. Prosser, J. A. Losonczi, I. V. Shiyankovskaya, *J. Am. Chem. Soc.* **1998**, *120*, 11010.
- [18] H. Wang, M. Eberstadt, E. T. Olejniczak, R. P. Meadows, S. W. Fesik, *J. Biomol. NMR* **1998**, *12*, 443.
- [19] M. Ottiger, A. Bax, *J. Biomol. NMR* **1999**, *13*, 187.
- [20] K. Fleming, D. Gray, S. Prasanna, S. Matthews, *J. Am. Chem. Soc.* **2000**, *122*, 5224.
- [21] M. Rückert, G. Otting, *J. Am. Chem. Soc.* **2000**, *122*, 7793.
- [22] G. M. Clore, M. R. Starich, A. M. Gronenborn, *J. Am. Chem. Soc.* **1998**, *120*, 10571.
- [23] B. E. Ramirez, A. Bax, *J. Am. Chem. Soc.* **1998**, *120*, 9106.
- [24] H. M. Al-Hashimi, H. Valafar, M. Terrell, E. R. Zartler, M. K. Eidsness, J. H. Prestegard, *J. Magn. Reson.* **2000**, *143*, 402.
- [25] G. A. Mueller, W. Y. Choy, D. W. Yang, J. D. Forman-Kay, R. A. Venters, L. E. Kay, *J. Mol. Biol.* **2000**, *300*, 197.
- [26] G. A. Mueller, W. Y. Choy, N. R. Skrynnikov, L. E. Kay, *J. Biomol. NMR* **2000**, *18*, 183.
- [27] C. A. Fowler, F. Tian, H. M. Al-Hashimi, J. H. Prestegard, *J. Mol. Biol.* **2000**, *304*, 447.
- [28] J.-C. Hus, D. Marion, M. Blackledge, *J. Mol. Biol.* **2000**, *298*, 927.
- [29] J.-C. Hus, D. Marion, M. Blackledge, *J. Am. Chem. Soc.* **2001**, *123*, 1541.
- [30] P. M. Bowers, C. E. M. Strauss, D. Baker, *J. Biomol. NMR* **2000**, *18*, 311.
- [31] F. Delaglio, G. Kontaxis, A. Bax, *J. Am. Chem. Soc.* **2000**, *122*, 2142.
- [32] M. Andrec, P. Du, R. M. Levy, *J. Biomol. NMR* **2001**, *21*, 335.
- [33] C. A. Rohl, D. Baker, *J. Am. Chem. Soc.* **2002**, *124*, 2723.
- [34] M. Zweckstetter, A. Bax, *J. Am. Chem. Soc.* **2001**, *123*, 9490.
- [35] F. Tian, H. Valafar, J. H. Prestegard, *J. Am. Chem. Soc.* **2001**, *123*, 11791.
- [36] A. W. Giesen, S. W. Homans, J. M. Brown, *J. Biomol. NMR* **2003**, *25*, 63.
- [37] S. Grzesiek, J. Anglister, H. Ren, A. Bax, *J. Am. Chem. Soc.* **1993**, *115*, 4369.
- [38] P. E. Coughlin, F. E. Anderson, E. J. Oliver, J. M. Brown, S. W. Homans, S. Pollak, J. W. Lustbader, *J. Am. Chem. Soc.* **1999**, *121*, 11871.
- [39] A. W. Giesen, L. C. Bae, C. L. Barrett, J. A. Chyba, M. M. Chaykovsky, M. C. Cheng, J. H. Murray, E. J. Oliver, S. M. Sullivan, J. M. Brown, F. W. Dahlquist, S. W. Homans, *J. Biomol. NMR* **2001**, *19*, 255.
- [40] M. K. Rosen, K. H. Gardner, R. C. Willis, W. E. Parris, T. Pawson, L. E. Kay, *J. Mol. Biol.* **1996**, *263*, 627.
- [41] K. H. Gardner, L. E. Kay, *J. Am. Chem. Soc.* **1997**, *119*, 7599.
- [42] N. K. Goto, K. H. Gardner, G. A. Mueller, R. C. Willis, L. E. Kay, *J. Biomol. NMR* **1999**, *13*, 369.
- [43] N. K. Goto, L. E. Kay, *Curr. Opin. Struct. Biol.* **2000**, *10*, 585.
- [44] Z. R. Wu, A. Bax, *J. Am. Chem. Soc.* **2002**, *124*, 9672.
- [45] B. Meyer, T. Peters, *Angew. Chem.* **2003**, *115*, 890; *Angew. Chem. Int. Ed.* **2003**, *42*, 864.

- [46] S. B. Shuker, P. J. Hajduk, R. P. Meadows, S. W. Fesik, *Science* **1996**, 274, 1531.
- [47] P. J. Hajduk, R. P. Meadows, S. W. Fesik, *Q. Rev. Biophys.* **1999**, 32, 211.
- [48] P. J. Hajduk, T. Gerfin, J. M. Boehlen, M. Haberli, D. Marek, S. W. Fesik, *J. Med. Chem.* **1999**, 42, 2315.
- [49] F. Abbate, L. Franzoni, F. Lohr, C. Lucke, E. Ferrari, R. T. Sorbi, H. Ruterjans, A. Spinsi, *J. Biomol. NMR* **1999**, 15, 187.
- [50] Z. Böcskei, C. R. Groom, D. R. Flower, C. E. Wright, S. E. V. Phillips, A. Cavaggioni, J. B. C. Findlay, A. C. T. North, *Nature* **1992**, 360, 186.
- [51] D. E. Timm, L. J. Baker, H. Mueller, L. Zidek, M. V. Novotny, *Protein Sci.* **2001**, 10, 997.
- [52] A. Medek, P. J. Hajduk, J. Mack, S. W. Fesik, *J. Am. Chem. Soc.* **2000**, 122, 1241.
- [53] L. Zidek, M. J. Stone, S. M. Lato, M. D. Pagel, Z. S. Miao, A. D. Ellington, M. V. Novotny, *Biochemistry* **1999**, 38, 9850.
- [54] C. Dalvit, P. Floersheim, M. G. M. Zurini, A. Widmer, *J. Biomol. NMR* **1999**, 14, 23.
- [55] J. Fejzo, C. A. Lepre, J. W. Peng, G. W. Bemis, Ajay, M. A. Murcko, J. M. Moore, *Chem. Biol.* **1999**, 6, 755.
- [56] P. J. Hajduk, D. J. Augeri, J. Mack, R. Mendoza, J. G. Yang, S. F. Betz, S. W. Fesik, *J. Am. Chem. Soc.* **2000**, 122, 7898.
- [57] P. J. Hajduk, E. T. Olejniczak, S. W. Fesik, *J. Am. Chem. Soc.* **1997**, 119, 12257.
- [58] B. Meyer, T. Weimar, T. Peters, *Eur. J. Biochem.* **1997**, 246, 705.
- [59] M. Mayer, B. Meyer, *Angew. Chem.* **1999**, 111, 1902; *Angew. Chem. Int. Ed.* **1999**, 38, 1784.
- [60] H. Takahashi, T. Nakanishi, K. Kami, Y. Arata, I. Shimada, *Nat. Struct. Biol.* **2000**, 7, 220.
- [61] W. Jahnke, P. Floersheim, C. Ostermeier, X. C. Zhang, R. Hemmig, K. Hurth, D. P. Uzunov, *Angew. Chem.* **2002**, 114, 3570; *Angew. Chem. Int. Ed.* **2002**, 41, 3420.
- [62] A. H. Siriwardena, F. Tian, S. Noble, J. H. Prestegard, *Angew. Chem.* **2002**, 114, 3604; *Angew. Chem. Int. Ed.* **2002**, 41, 3454.
- [63] J. Fiaux, E. B. Bertelsen, A. L. Horwich, K. Wüthrich, *Nature* **2002**, 418, 207.
- [64] K. Pervushin, R. Riek, G. Wider, K. Wüthrich, *Proc. Natl. Acad. Sci. USA* **1997**, 94, 12366.
- [65] G. Otting, H. Senn, G. Wagner, K. Wüthrich, *J. Magn. Reson.* **1986**, 70, 500.
- [66] G. Otting, K. Wüthrich, *J. Magn. Reson.* **1989**, 85, 586.
- [67] C. Zwahlen, P. Legault, S. J. F. Vincent, J. Greenblatt, R. Konrat, L. E. Kay, *J. Am. Chem. Soc.* **1997**, 119, 6711.
- [68] A. M. Petros, R. T. Gampe, G. Gemmecker, P. Neri, T. F. Holzman, R. Edalji, J. Hochlowski, M. Jackson, J. McAlpine, J. R. Luly, T. Pilotmatias, S. Pratt, S. W. Fesik, *J. Med. Chem.* **1991**, 34, 2925.
- [69] A. M. Petros, G. Gemmecker, P. Neri, E. T. Olejniczak, D. Nettekheim, R. X. Xu, E. G. Gubbins, H. Smith, S. W. Fesik, *J. Med. Chem.* **1992**, 35, 2467.
- [70] D. G. Low, M. A. Probert, G. Embleton, K. Seshadri, R. A. Field, S. W. Homans, J. Windust, P. J. Davis, *Glycobiology* **1997**, 7, 373.
- [71] M. Pellecchia, D. Meininger, Q. Dong, E. Chang, R. Jack, D. S. Sem, *J. Biomol. NMR* **2002**, 22, 165.
- [72] H. Shimizu, A. Donohue-Rolfe, S. W. Homans, *J. Am. Chem. Soc.* **1999**, 121, 5815.
- [73] P. J. Bolon, H. M. Al-Hashimi, J. H. Prestegard, *J. Mol. Biol.* **1999**, 293, 107.
- [74] H. M. Al-Hashimi, P. J. Bolon, J. H. Prestegard, *J. Magn. Reson.* **2000**, 142, 153.
- [75] M. Zweckstetter, A. Bax, *J. Am. Chem. Soc.* **2000**, 122, 3791.
- [76] E. T. Olejniczak, R. P. Meadows, H. Wang, M. L. Cai, D. G. Nettekheim, S. W. Fesik, *J. Am. Chem. Soc.* **1999**, 121, 9249.
- [77] F. Tian, P. J. Bolon, J. H. Prestegard, *J. Am. Chem. Soc.* **1999**, 121, 7712.
- [78] P. J. Bolon, J. H. Prestegard, *J. Am. Chem. Soc.* **1998**, 120, 9366.
- [79] W. Peti, C. Griesinger, *J. Am. Chem. Soc.* **2000**, 122, 3975.
- [80] Z. G. Li, S. Raychaudhuri, A. J. Wand, *Protein Sci.* **1996**, 5, 2647.
- [81] D. W. Yang, L. E. Kay, *J. Mol. Biol.* **1996**, 263, 369.
- [82] D. Yang, Y.-K. Mok, J. D. Forman-Kay, N. Farrow, L. E. Kay, *J. Mol. Biol.* **1997**, 272, 790.
- [83] M. Akke, R. Brüschweiler, A. G. Palmer, *J. Am. Chem. Soc.* **1993**, 115, 9832.
- [84] A. G. Palmer, *Annu. Rev. Biophys. Biomol. Struct.* **2001**, 30, 129.
- [85] G. Lipari, A. Szabo, *J. Am. Chem. Soc.* **1982**, 104, 4546.
- [86] C. Bracken, P. A. Carr, J. Cavanagh, A. G. Palmer, *J. Mol. Biol.* **1999**, 285, 2133.
- [87] J. Evenas, S. Forsen, A. Malmendal, M. Akke, *J. Mol. Biol.* **1999**, 289, 603.
- [88] J. O. Wrabl, D. Shortle, T. B. Woolf, *Proteins Struct. Funct. Genet.* **2000**, 38, 123.
- [89] L. Zidek, M. V. Novotny, M. J. Stone, *Nat. Struct. Biol.* **1999**, 6, 1118.
- [90] A. L. Lee, P. F. Flynn, A. J. Wand, *J. Am. Chem. Soc.* **1999**, 121, 2891.
- [91] D. R. Muhandiram, T. Yamazaki, B. D. Sykes, L. E. Kay, *J. Am. Chem. Soc.* **1995**, 117, 11536.
- [92] R. Ishima, A. P. Petkova, J. M. Louis, D. A. Torchia, *J. Am. Chem. Soc.* **2001**, 123, 6164.
- [93] R. Ishima, J. M. Louis, D. A. Torchia, *J. Biomol. NMR* **2001**, 21, 167.
- [94] D. M. LeMaster, *J. Am. Chem. Soc.* **1999**, 121, 1726.
- [95] A. Mittermaier, L. E. Kay, J. D. Forman-Kay, *J. Biomol. NMR* **1999**, 13, 181.
- [96] A. L. Lee, S. A. Kinnear, A. J. Wand, *Nat. Struct. Biol.* **2000**, 7, 72.
- [97] J. Cavanagh, M. Akke, *Nat. Struct. Biol.* **2000**, 7, 11.
- [98] J. D. Dunitz, *Chem. Biol.* **1995**, 2, 709.
- [99] D. H. Williams, D. P. O'Brien, B. Bardsley, *J. Am. Chem. Soc.* **2001**, 123, 737.
- [100] C. T. Calderone, D. H. Williams, *J. Am. Chem. Soc.* **2001**, 123, 6262.
- [101] V. P. Denisov, K. Venu, J. Peters, H. D. Horlein, B. Halle, *J. Phys. Chem. B* **1997**, 101, 9380.